

Electro Deposition of silver sulphide (Ag_2S) and cerium doped silver sulphide (Ce: Ag_2S) thin films for structural properties investigation

¹Lois Ugomma Okafor, ²Donald N. Okoli, ³Azubike J. Ekpunobi

^{1,2,3}Department of Physics and industrial physics, Nnamdi Azikiwe University, Awka Anambra State, Nigeria

*Corresponding Author's E-mail: lu.okafor@unizik.edu.ng

Abstract

In this research, Ag_2S and Cerium doped Ag_2S thin film were successfully synthesized and characterized for structural properties analysis for optoelectronics devices application. Deposition of thin film made from cerium-doped silver chalcogenide (Ce: Ag_2S) was conducted at room temperature. Crystal structural analysis of the deposited thin film was done using x – ray diffractometer machine. Various bath parameters including deposition time, pH level, and molar concentration of the cerium precursor were adjusted to optimize their impact on the structural characteristics of this thin film. The effects of percentage concentration of cerium dopant, deposition time and pH on the structural properties of Ag_2S and Cerium doped Ag_2S thin films were reported in this work. From the experimental investigation, increase in intensity of the diffraction spectra was observed as dopant concentration increased from 5% to 10%. The diffractogram exhibits distinct peaks corresponding to specific crystallographic planes, indicating changes in lattice parameters due to varying deposition times which shows that that longer deposition times lead to better crystal quality with fewer lattice defects and larger crystallites. The investigation also revealed that lowest pH tested leads to a good balance of structural properties. The obtained results in this study revealed good results which are comparable with results obtained by other researchers in literature. These results obtained suggest the possibility of using the material in optoelectronics devices like LEDs, solar cells, transducers, and photodetectors.

Keywords: Electro deposition, Cerium doped silver sulphide(Ce: Ag_2S), X– ray diffractometer machine

1. Introduction

The increasing demand for efficient, cost-effective, and scalable materials for optoelectronic, photovoltaic, and sensor applications has intensified research into semiconducting thin films. Among these silver chalcogenides, silver sulphide (Ag_2S) has gained attention due to their favorable optical and electronic properties, such as narrow band gaps, high absorption coefficients, and good environmental stability. However, the performance of undoped silver chalcogenide thin films is often limited by inherent structural defects, suboptimal crystallinity, poor surface morphology, and restricted tunability of optical properties, all of which hinder their applicability in advanced technologies. Additionally, the properties of these materials are highly sensitive to deposition parameters, and systematic studies that correlate growth conditions with functional performance are limited. Cerium, a rare-earth element with unique electronic characteristics, offers potential as a dopant to enhance crystallinity, reduce defect densities, and modulate the optical and structural behavior of silver chalcogenide films. Despite this potential, the effects of cerium incorporation on the microstructural, optical, and morphological properties of Ag_2S , thin films synthesized via electrodeposition have not been comprehensively explored. This study addresses this gap by investigating how cerium doping and deposition parameters influence the quality and functional characteristics of these thin films, with the goal of optimizing their properties for use in high-performance optoelectronic and energy-conversion devices. This study is significant in addressing the growing need for high-performance, low-cost, and scalable materials for optoelectronic and energy-related technologies.

Specifically, the main aim of this study is to investigate the effects of dopant concentration, deposition time and the pH of the electrolytic bath on the structural properties of cerium doped silver sulphide for possible device applications. The objectives of the study are fabrication of thin films of Ce:Ag₂S by electro deposition method, optimization deposition parameters such as concentration of dopant (Cerium), deposition potential and pH of the electrolytic medium, characterization and analysis of electro deposited Ce:Ag₂S thin films. Silver sulphide (Ag₂S) thin films are an important class of chalcogenide semiconductors, known for their p-type and n-type conductivity, and are widely studied for various applications. They belong to the I-VI compound semiconductors with a monoclinic crystal structure. The films can be deposited using various techniques, including solution growth, electrodeposition, and chemical bath deposition. Chalcogenide thin films have been investigated and explored by many researchers in the last decades to broaden their application in optical, electronic, and optoelectronic device sectors. Chalcogenide compounds, such as Ag₂S, have become greatly important due to their general applications in different fields, Yadu et al., (2015). Ag₂S is among the I-VI compound semiconductor which has a monoclinic crystal structure. Ag₂S thin films are useful components in a range of modern technologies, like in photoconductive, Xue et al., (2019).

Doping foreign elements is the most productive and efficient way to improve their structural ability, optical characteristics, and electronic approaches. As a result of that, metal doping has an enormous impact on the aspects and understanding of the mechanism inside the matrix. In this present study, we present the synthesis and characterization of Ag₂S and Ce doped Ag₂S thin film for structural properties investigation. Electrodeposition method was used to deposit chalcogenide thin film semiconductor alloys of Cerium doped silver sulphide on fluorine doped tin oxide (FTO) conductive glass substrate to study the effect of cerium ions, deposition time and pH on the structural properties for possible device applications. This deposition technique presents several advantages, such as precise management of film characteristics, the ability to coat conformally, faster deposition rates, cost-effective, suitability for multicomponent setups, eco-friendliness and flexibility (Yu et al., 2023, Ruiz et al., 2022). These factors make it a preferred choice for thin film fabrication in various fields. Many researchers such as (Yimamu et al., 2023, Park et al., 2022, Sawant et al., 2022, Guessan et al., 2023, Mohapi et al., 2023, Tanwar et al., 2023, Hwang et al., 2024, Rodriguez et al., 2020) have reported the use of electrodeposition in the synthesis of thin films. The motivation for this work arose from the fact that there is no literature available on the effects of deposition time, pH and dopant concentration on the structural properties of electrodeposited cerium doped silver sulphide (Ce:Ag₂S) thin films. The purpose of this research is to address this literature gap by investigating the effects of dopant concentration, deposition time and pH on the structural properties of Ce:Ag₂S thin films synthesized via electrodeposition for optoelectronics application.

2.0 Materials and methods

2.1 Materials used

Materials that were used in this work include apparatus and reagents.

2.1.1 Apparatus

The following apparatus and equipment were used during the experiment. Beakers (100 mL) were used for mixing solutions. Fluorine-doped tin oxide (FTO) glass slide (15 Ω/sq) was used as the substrate or working electrode. An electronic compact scale (Atom: model 110C, capacity – 750 g, accuracy - 0.01 g) was used for determining the weight of reagents. A magnetic stirrer with hotplate (Labsience 85–2) was used for stirring the solutions. A DC power supply served as a source of electric energy (potential difference). Digital multimeters such as the DT9201A CE and Mastech MY60 were utilized for the measurement of current and voltage. Platinum foil served as the counter electrode in this experiment. The Ag/AgCl electrode functioned as the reference electrode. An ultrasonic bath was employed for degreasing the substrates. An electrically heated thermostatic dry box (oven), model DH69101, was employed for drying purposes. An X-ray diffraction machine was used for structural properties analysis.

2.1.2. Reagents

Reagents used for electrodeposition of cerium-doped silver sulphide (Ce:Ag₂S) were as follows: Silver trioxonitrate (V) was used as a precursor for silver ion. Cerium tetraoxosulphate (VI) tetrahydrate was used as a precursor for cerium ion (dopant ion). Sodium thiosulphate was used as a precursor for sulphur ion. Ethylene diamine tetraacetic acid (EDTA) was used as a complexing agent. Tetraoxosulphate (VI) acid was used as a pH adjuster.

2.2. Material Preparation

2.2.1 .Electrodeposition of silver sulphide (Ag_2S) and cerium doped silver sulphide ($Ce: Ag_2S$) thin films

For electrodeposition of silver sulphide thin film on FTO substrate, aqueous electrolytic bath composed of 20 ml of 0.05M of silver trioxonitrate (V) was used to dissolve 0.7 g of EDTA to form complex solution. After stirring for 5 minutes, 20 ml of 0.05M of sodium thiosulphate was added to the solution. The mixture was stirred for another 10 minute to totally dissolve the EDTA. The three electrodes were immersed into the bath containing the electrolytic solution and 1.5 volts was allowed to pass through the setup for 120 seconds (2 minutes). After the allowed time, dark film of Ag_2S was found to be deposited on the conductive surface of the FTO substrate. The deposited Ag_2S thin film was heat-treated at 100 °C for 10 minute to remove water and increase the crystallinity of the deposited thin film. The mechanism of the formation of silver sulphide and cerium doped silver sulphide is shown in equation (1) and (2).



2.2.2. Optimization of Ce ion concentration for Ce: Ag_2S thin films

For the deposition of Ce doped Ag_2S thin films, 0.05 M of cerium (IV) tetraoxo sulphate tetrahydrate was used. Similar procedure used for deposition of silver sulphide thin film was adopted but with addition of different volume concentrations of 0.05 M of cerium (IV) tetraoxo sulphate tetra hydrate as shown in Table 1. Four samples with different dopant volume concentrations of 1 ml, 2 ml, 3 ml and 4 ml were fabricated.

Table 1: Bath parameter for deposition of Ag_2S and Ce doped Ag_2S thin films

| 0.05 M of $AgNO_3$ | 0.05 M of $Na_2S_2O_3$ | 0.05 M of $CeSO_4 \cdot 4H_2O$ | of EDTA | Applied Voltage | Time |
|--------------------|------------------------|--------------------------------|-----------|-----------------|--------|
| Vol. (ml) | Vol. (ml) | Vol. (ml) | Conc. (g) | (volts) | (sec.) |
| 20.00 | 20.00 | - | 0.70 | 1.50 | 120 |
| 20.00 | 20.00 | 1.00 | 0.70 | 1.50 | 120 |
| 20.00 | 20.00 | 2.00 | 0.70 | 1.50 | 120 |
| 20.00 | 20.00 | 3.00 | 0.70 | 1.50 | 120 |
| 20.00 | 20.00 | 4.00 | 0.70 | 1.50 | 120 |

2.2.3. Optimization of deposition time for Ce: Ag_2S thin films

For time optimization of Ce doped Ag_2S thin films, similar procedure used for deposition of cerium doped silver sulphide thin film was adopted. The 0.05 M of silver trioxonitrate (V) and 0.05 M of cerium (IV) tetraoxosulphatetetrahydrate, 0.70 g of EDTA and 0.05 M of sodium thiosulphate were used for the deposition. Five films were deposited at time interval of 30 seconds, 60 seconds, 90 seconds, 120 seconds and 150 seconds. Table 2 shows the constituent of the electrolytic baths used for the deposition of Ce doped Ag_2S at varying deposition time.

Table 2: Bath parameter for time optimized Ce: Ag_2S thin films

| 0.05 M of $AgNO_3$ | 0.05 M of $Na_2S_2O_3$ | 0.05 M of $CeSO_4 \cdot 4H_2O$ | of EDTA | Applied Voltage | Time |
|--------------------|------------------------|--------------------------------|-----------|-----------------|--------|
| Vol. (ml) | Vol. (ml) | Vol. (ml) | Conc. (g) | (volts) | (sec.) |
| 20.00 | 20.00 | 2.00 | 0.70 | 1.50 | 30 |
| 20.00 | 20.00 | 2.00 | 0.70 | 1.50 | 60 |
| 20.00 | 20.00 | 2.00 | 0.70 | 1.50 | 90 |
| 20.00 | 20.00 | 2.00 | 0.70 | 1.50 | 120 |
| 20.00 | 20.00 | 2.00 | 0.70 | 1.50 | 150 |

2.2.4. Optimization of deposition pH for Ce: Ag_2S thin films

For pH optimization of Ce doped Ag_2S thin films, similar procedures used for deposition of cerium doped silver sulphide thin film were maintained. The 0.05 M of silver trioxonitrate (V) and 0.05 M of cerium (IV) tetraoxosulphatetetrahydrate, 0.70 g of EDTA and 0.05 M of sodium thiosulphate were used for the deposition. Five films were deposited with different mass of EDTA. EDTA quantity used were 0.5 g, 0.6 g, 0.7 g, 0.8 g and finally 0.9 g. Table 3 shows the constituent of the electrolytic baths used for the deposition of Ce doped Ag_2S at varying pH.

Table 3: Bath parameter for pH optimized Ce: Ag₂S thin films

| 0.05 M of AgNO ₃ | 0.05 M of Na ₂ S ₂ O ₃ | 0.05 M of CeSO ₄ ·4H ₂ O | EDTA | Applied Voltage | Time |
|-----------------------------|---|--|-----------|-----------------|--------|
| Vol. (ml) | Vol. (ml) | Vol. (ml) | Conc. (g) | (volts) | (sec.) |
| 20.00 | 20.00 | 2.00 | 0.50 | 1.50 | 120 |
| 20.00 | 20.00 | 2.00 | 0.60 | 1.50 | 120 |
| 20.00 | 20.00 | 2.00 | 0.70 | 1.50 | 120 |
| 20.00 | 20.00 | 2.00 | 0.80 | 1.50 | 120 |
| 20.00 | 20.00 | 2.00 | 0.90 | 1.50 | 120 |

2.2.5. Electrodeposition of thin films

The experimental arrangement depicted in Figure 1 as given by (Okoliet *al.*, 2022) illustrates the setup for electrodeposition, comprising the electrolyte, power supply unit, and electrodes. It adopts a three-electrode configuration for depositing thin films onto conducting substrates. The conducting substrate, specifically FTO, was used as the cathode or working electrode. A platinum electrode functioned as the anode or counter electrode, while a silver/silver chloride (Ag/AgCl) electrode served as the reference electrode. The energy supply for the electrodeposition setup is provided by a Dazheng digital DC-power supply unit, specifically the PS-1502A model. Two digital multimeters, the DT9201A CE and the highly sensitive Mastech: MY60 were employed for measuring voltage and current, respectively. The Mastech: MY60 multimeter is capable of measuring currents within the range of 10^{-6} A.

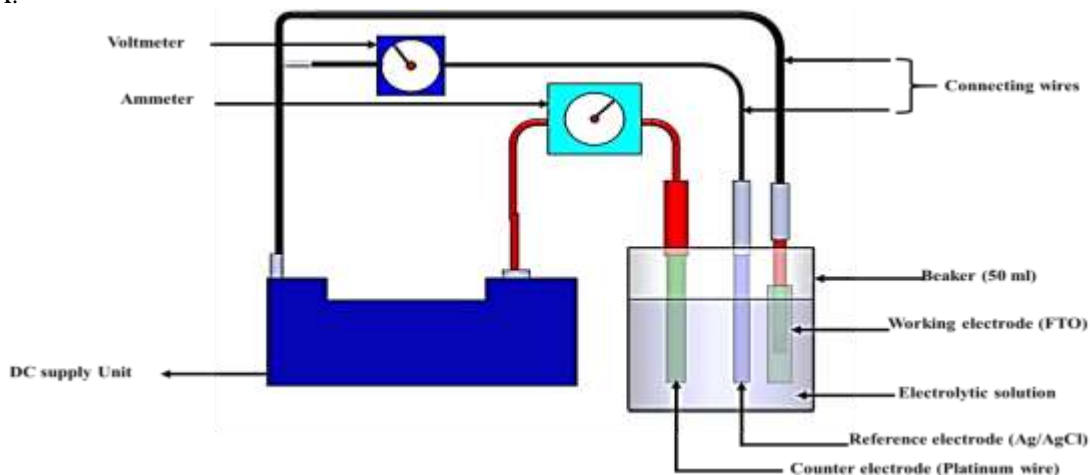


Figure 1: Schematic diagram of the electrodeposition experimental set – up (Okoli *et al.*, 2022)

Deposition of thin film made from cerium-doped silver chalcogenides (Ce:Ag₂S) was conducted at room temperature. Various bath parameters including deposition time, pH level, and molar concentration of the cerium precursor were adjusted to optimize their impact on the optical, structural, compositional, morphological, and electrical characteristics of these thin films.

2.3. Structural characterization

Crystal structural analyses of the deposited thin films were done using x – ray diffractometer machine. Empyrean diffractometer (DY 674) located at Nigeria Geological Research Laboratory (NGRL) Kaduna, Kaduna State and Buker D8 high resolution diffractometer at Material Research Department, Themba Labs, Johannesburg, South Africa were employed to study the structural properties of these films. From the x – ray diffraction pattern obtained, other structural properties such as d – spacing, full width at half maximum (FWHM) were obtained. The crystallite sizes and micro strains of the films were evaluated using Scherer's formula. Debye – Scherer's formula for calculating crystallite sizes of a thin film material is given by (Ravindranah *et al.*, 2016; Okorieimoh, *et al.*, 2019) as

$$D = \frac{0.9\lambda}{\beta \cos \theta} \quad 3$$

The dislocation density (δ) of thin films can be estimated using expression as provided by Anbarasi *et al.*, (2016); Hadri *et al.*, (2015) in equation (4).

$$\delta = \frac{1}{D^2} \quad 4$$

3.0 Result and Discussion

3.1 Structural properties of Ag₂S and Ce doped Ag₂S thin films

(a) Variation of structural properties with percentage concentration of cerium dopant

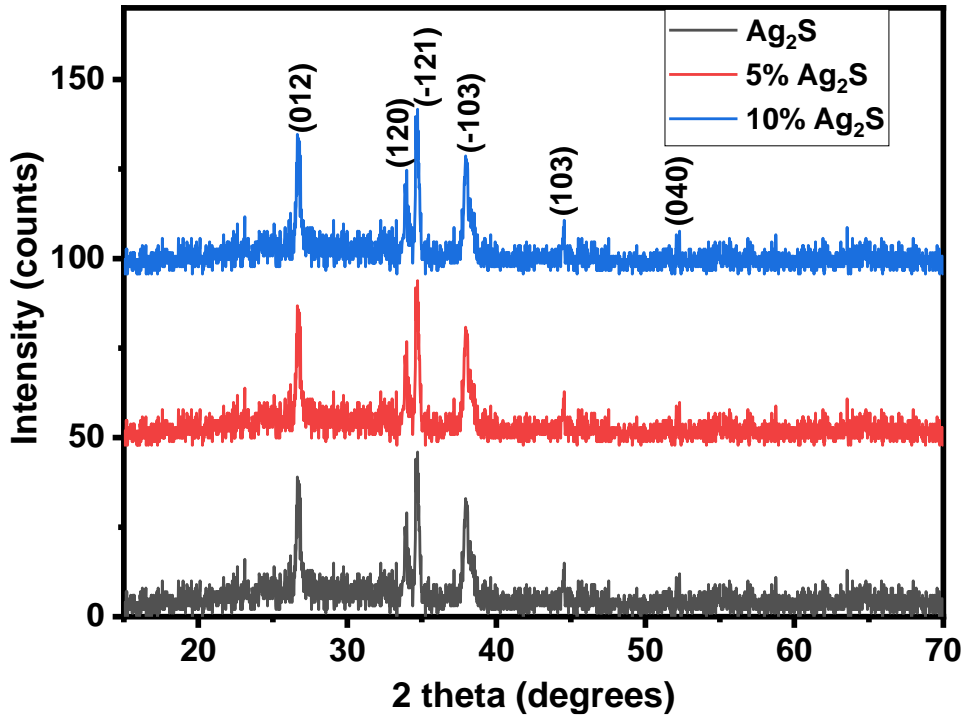


Figure 2: Diffractogram of Ag₂S and cerium doped Ag₂S deposited with different percentage concentration of dopant

Figure 2 and table 4 show the diffractogram and structural parameters of Ag₂S and cerium doped Ag₂S thin films deposited at different doping concentration of 5% and 10% respectively. The X-ray diffraction analysis of Ag₂S and cerium-doped Ag₂S reveals significant structural modifications due to doping. The diffractogram exhibits distinct peaks corresponding to specific crystallographic planes, with observed shifts and intensity variations indicating changes in lattice parameters. The peaks for pure Ag₂S are identified at the angles 26.712°, 33.949°, 34.692°, 38.027°, 44.470°, and 52.812°, corresponding to the Miller indices (012), (120), (121), (-103), (103), and (040) respectively. The diffractogram matches the JCPDS file number 00-014-0072, which is associated with the mineral name Acanthite and the monoclinic phase. The calculated crystallite sizes for pure Ag₂S range from 14.62 nm to 82.53 nm, with the smallest crystallites observed at 38.027° (14.62 nm) and the largest at 44.470° (82.53 nm). The micro-strain values for pure Ag₂S, varying between 1.12×10^{-3} and 7.27×10^{-3} , indicate that higher strain correlates with smaller crystallite sizes. The dislocation densities range from $1.47 \times 10^{-5} \text{ lines/nm}^2$ to $4.68 \times 10^{-3} \text{ lines/nm}^2$. Increase in intensity of the diffraction spectra was observed as dopant concentration increased from 5% to 10%. Cerium affects crystallite size or strain of cerium doped silver sulphide because cerium ions have different ionic radii compared to the silver ions.

Table 4: Structural parameters of Ag₂S and cerium doped Ag₂S thin films

| Doping Level | 2 Theta (°) | hkl | FWHM (°) | Crystallite Size (nm) | Micro-strain (ε) × 10 ⁻³ | Dislocation Density × 10 ⁻³ lines/nm ² |
|--------------------------|----------------|------|----------|-----------------------|-------------------------------------|--|
| Ag ₂ S | 26.712 | 012 | 0.369 | 22.15 | 6.80 | 2.04 |
| | 33.949 | 120 | 0.392 | 21.17 | 5.57 | 2.23 |
| | 34.692 | -121 | 0.296 | 28.13 | 4.14 | 1.27 |
| | 38.027 | -103 | 0.574 | 14.62 | 7.27 | 4.68 |
| | 44.470 | 103 | 0.105 | 82.53 | 1.12 | 0.02 |
| | 52.812 | 040 | 0.296 | 30.07 | 2.59 | 1.11 |
| | Average | | | 33.11 | 1.93 | 4.58 |
| 5% Ce:Ag ₂ S | 26.712 | 012 | 0.369 | 22.11 | 6.81 | 2.05 |
| | 33.949 | 120 | 0.394 | 21.08 | 5.59 | 2.25 |
| | 34.692 | -121 | 0.296 | 28.07 | 4.14 | 1.27 |
| | 38.028 | -103 | 0.575 | 14.58 | 7.29 | 4.70 |
| | 44.511 | 103 | 0.152 | 56.35 | 1.64 | 0.315 |
| | 52.359 | 040 | 0.196 | 45.36 | 1.72 | 0.486 |
| | Average | | | 31.26 | 1.93 | 4.58 |
| 10% Ce:Ag ₂ S | 26.712 | 012 | 0.369 | 22.11 | 6.81 | 2.05 |
| | 33.949 | 120 | 0.394 | 21.08 | 5.59 | 2.25 |
| | 34.692 | -121 | 0.296 | 28.07 | 4.14 | 1.27 |
| | 38.028 | -103 | 0.575 | 14.58 | 7.29 | 4.70 |
| | 44.511 | 103 | 0.152 | 56.35 | 1.64 | 0.315 |
| | 52.459 | 040 | 0.196 | 45.36 | 1.72 | 0.486 |
| | Average | | | 31.26 | 1.93 | 4.58 |

For Ag₂S doped with 5% cerium, the peak angles are 26.712°, 33.949°, 34.692°, 38.028°, 44.511°, and 52.359°. The crystallite sizes for 5% cerium-doped Ag₂S range from 14.58 nm to 56.35 nm, the micro-strain varies from 1.64×10^{-3} to 7.29×10^{-3} , and the dislocation density ranges from $3.15 \times 10^{-4} \text{ lines/nm}^2$ to $4.70 \times 10^{-3} \text{ lines/nm}^2$. Similarly, for Ag₂S doped with 10% cerium, the peak angles are 26.712°, 33.949°, 34.692°, 38.028°, 44.511°, and 52.459°. The crystallite sizes for 10% cerium-doped Ag₂S range from 14.58 nm to 56.35 nm, the micro-strain varies from 1.64×10^{-3} to 7.29×10^{-3} , and the dislocation density ranges from $3.15 \times 10^{-4} \text{ lines/nm}^2$ to $4.70 \times 10^{-3} \text{ lines/nm}^2$. The slight variations in the micro strain indicate that higher strain correlates with smaller crystallite sizes, implying that doping induces lattice distortions. Changes in dislocation densities further confirm the impact of doping on crystal quality, with higher dislocation densities associated with increased doping levels, leading to more defects within the lattice. The average values of crystallite size, dislocation density and microstrain for pure Ag₂S are 33.11 nm, $1.89 \times 10^{-3} \text{ lines/nm}^2$ and 4.58×10^{-3} respectively. For 5% and 10% cerium-doped Ag₂S, the average values are approximately the same with values of 31.26 nm, $1.85 \times 10^{-3} \text{ lines/nm}^2$ and 4.53×10^{-3} . These results collectively suggest that cerium doping significantly alters the structural properties of Ag₂S, affecting both crystallite size and lattice integrity. These results collectively suggest that cerium doping significantly alters the structural properties of Ag₂S, affecting both crystallite size and lattice integrity. The consistent FWHM values for both 5% and 10% cerium-doped samples indicate that higher doping levels induce similar levels of micro-strain and dislocation density, thereby affecting the overall crystal quality.

(b) Variation of structural properties with deposition time

Figure 3 and table 5 show the diffractogram and structural parameters of cerium doped Ag₂S thin films deposited at different deposition time. Ce doped Ag₂S deposited at different times (30 seconds, 90 seconds, and 150 seconds) reveals significant variations in structural properties with deposition time. The diffractogram exhibits distinct peaks corresponding to specific crystallographic planes, indicating changes in lattice parameters due to varying deposition times. The diffractogram matches the JCPDS reference file number 00-014-0072, which is associated with the mineral name Acanthite and the monoclinic phase. For the sample deposited at 30 seconds, the crystallite sizes range from 12.05 nm to 40.34 nm, with an average crystallite size of 23.94 nm. The dislocation densities vary between

$0.614 \times 10^{-3} \text{ lines/nm}^2$ and $6.89 \times 10^{-3} \text{ lines/nm}^2$, with an average dislocation density of $3.32 \times 10^{-3} \text{ lines/nm}^2$.

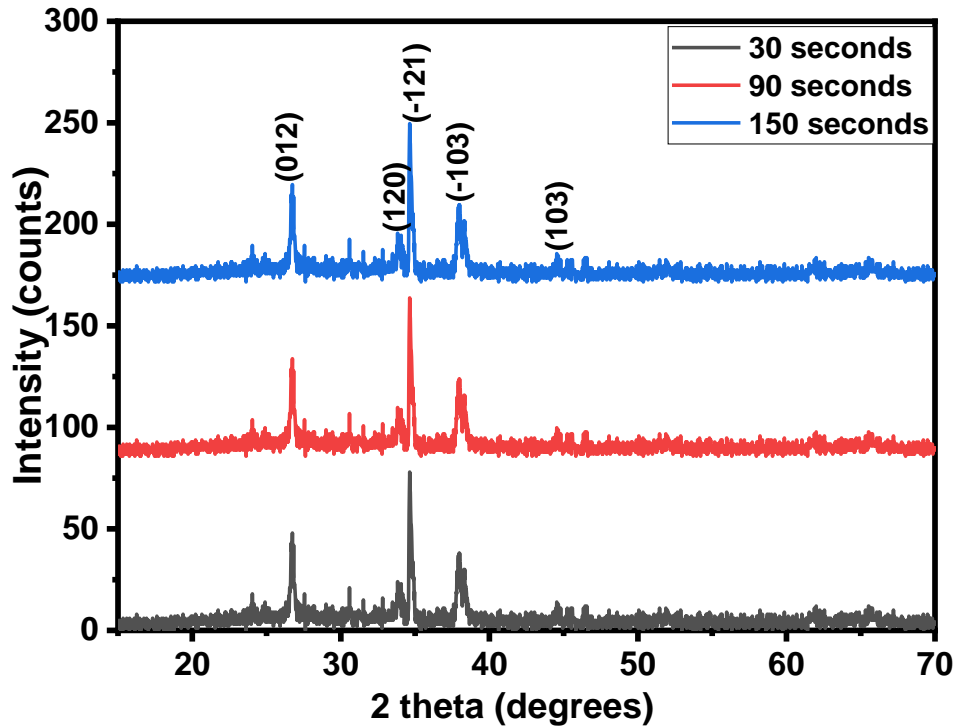


Figure 3: Diffractogram of Ag_2S and cerium doped Ag_2S deposited under different deposition time

Table 5: Structural parameters of cerium doped Ag_2S thin films deposited at different time

| Deposition Time | 2 Theta ($^\circ$) | hkl | FWHM ($^\circ$) | Crystallite Size (nm) | Micro-strain (ϵ) $\times 10^{-3}$ | Dislocation Density $\times 10^{-3} \text{ lines/nm}^2$ |
|-----------------|----------------------|------|-------------------|-----------------------|--|---|
| 30 seconds | 26.730 | 012 | 0.322 | 25.35 | 5.92 | 1.56 |
| | 33.821 | 120 | 0.699 | 12.05 | 6.5 | 6.89 |
| | 34.690 | -121 | 0.207 | 40.34 | 2.45 | 0.61 |
| | 38.076 | -103 | 0.679 | 12.5 | 6.14 | 6.40 |
| | 44.546 | 103 | 0.290 | 29.44 | 2.98 | 1.15 |
| | Average | | | | 23.94 | 4.80 |
| 90 seconds | 26.730 | 012 | 0.322 | 25.35 | 5.92 | 1.56 |
| | 33.751 | 120 | 0.599 | 14.04 | 5.57 | 5.07 |
| | 34.690 | -121 | 0.207 | 40.34 | 2.45 | 0.61 |
| | 38.076 | -103 | 0.679 | 12.5 | 6.14 | 6.40 |
| | 44.546 | 103 | 0.290 | 29.44 | 2.98 | 1.15 |
| | Average | | | | 24.33 | 4.61 |
| 150 seconds | 26.728 | 012 | 0.282 | 28.97 | 5.19 | 1.19 |
| | 33.788 | 120 | 0.416 | 20.23 | 3.87 | 2.44 |
| | 34.691 | -121 | 0.224 | 37.28 | 2.65 | 0.72 |
| | 38.076 | -103 | 0.647 | 13.11 | 5.86 | 5.82 |
| | 44.547 | 103 | 0.332 | 25.72 | 3.41 | 1.51 |
| | Average | | | | 25.46 | 4.20 |

The micro-strain values range from 2.45 to 6.50, with an average strain of 4.80. For the sample deposited at 90 seconds, the crystallite sizes range from 12.50 nm to 40.34 nm, with an average crystallite size of 24.33 nm. The dislocation densities for this sample vary between $0.614 \times 10^{-3} \text{ lines/nm}^2$ and $6.40 \times 10^{-3} \text{ lines/nm}^2$, with an average dislocation density of 2.96 lines/nm^2 . The micro-strain values range from 2.45×10^{-3} to 6.14×10^{-3} , with an average strain of 4.61×10^{-3} . Compared to the 30-second deposition, the 90-second sample shows a slight increase in average crystallite size and a minor decrease in average dislocation density and strain, indicating an improvement in crystal quality with longer deposition times.

For the sample deposited at 150 seconds, the crystallite sizes range from 13.11 nm to 37.28 nm, with an average crystallite size of 25.46 nm. The dislocation densities for this sample vary between 0.719×10^{-3} and $5.82 \times 10^{-3} \text{ lines/nm}^2$, with an average dislocation density of $2.34 \times 10^{-3} \text{ lines/nm}^2$. The micro-strain values range from 2.65×10^{-3} to 5.86×10^{-3} , with an average strain of 4.20×10^{-3} . The 150-second deposition time results in the largest average crystallite size and the lowest average dislocation density and strain among the three deposition times, suggesting that longer deposition times lead to better crystal quality with fewer lattice defects and larger crystallites.

(c) Variation of structural properties with concentration of pH

Table 6: Structural parameters of cerium doped Ag_2S thin films deposited at different pH

| pH | 2 Theta (°) | hkl | FWHM (°) | Crystallite Size (nm) | Dislocation Density $\times 10^{-3} \text{ lines/nm}^2$ | Micro-strain (ϵ) $\times 10^{-3}$ |
|------|----------------|------|----------|-----------------------|---|--|
| 3.23 | 26.711 | 012 | 0.299 | 28.543 | 1.227 | 5.491 |
| | 33.882 | 120 | 0.584 | 14.859 | 4.529 | 8.362 |
| | 34.770 | -121 | 0.297 | 29.321 | 1.163 | 4.133 |
| | 38.200 | -103 | 0.518 | 16.941 | 3.484 | 6.531 |
| | 44.555 | 103 | 0.729 | 12.301 | 6.608 | 7.764 |
| | Average | | | 20.393 | 3.402 | 6.456 |
| 3.15 | 26.741 | 012 | 0.249 | 34.280 | 0.851 | 4.567 |
| | 33.782 | 120 | 0.531 | 16.319 | 3.755 | 7.636 |
| | 34.760 | -121 | 0.297 | 29.320 | 1.163 | 4.134 |
| | 38.230 | -103 | 0.608 | 14.436 | 4.798 | 7.658 |
| | 44.675 | 103 | 0.439 | 20.439 | 2.98 | 4.661 |
| | Average | | | 22.959 | 2.592 | 5.731 |
| 3.04 | 26.631 | 012 | 0.299 | 28.538 | 1.228 | 5.508 |
| | 33.842 | 120 | 0.584 | 14.858 | 4.530 | 8.372 |
| | 34.620 | -121 | 0.297 | 29.309 | 1.164 | 4.152 |
| | 38.190 | -103 | 0.508 | 17.274 | 3.351 | 6.407 |
| | 44.755 | 103 | 0.339 | 26.476 | 1.427 | 3.592 |
| | Average | | | 23.291 | 2.340 | 5.606 |

The X-ray diffraction analysis of cerium-doped Ag_2S thin films deposited at different pH values of 3.23, 3.15, and 3.04 as shown in figure 4 reveals significant variations in structural properties with pH. The diffractogram exhibits distinct peaks corresponding to specific crystallographic planes, matched to the JCPDS reference file number 00-014-0072, associated with the mineral name Acanthite and the monoclinic phase. The Miller indices corresponding to the 2 theta angles mentioned for each thin film are shown in the graph of Figure 4. Detailed structural parameters for each sample are summarized in Table 6, highlighting the effects of pH on crystallite size, dislocation density, and lattice strain. The consistent appearance of these peaks across different pH values confirms the preservation of the monoclinic phase of Ag_2S , while the variation in peak intensity and width reflects the changes in crystallite size and structural quality.

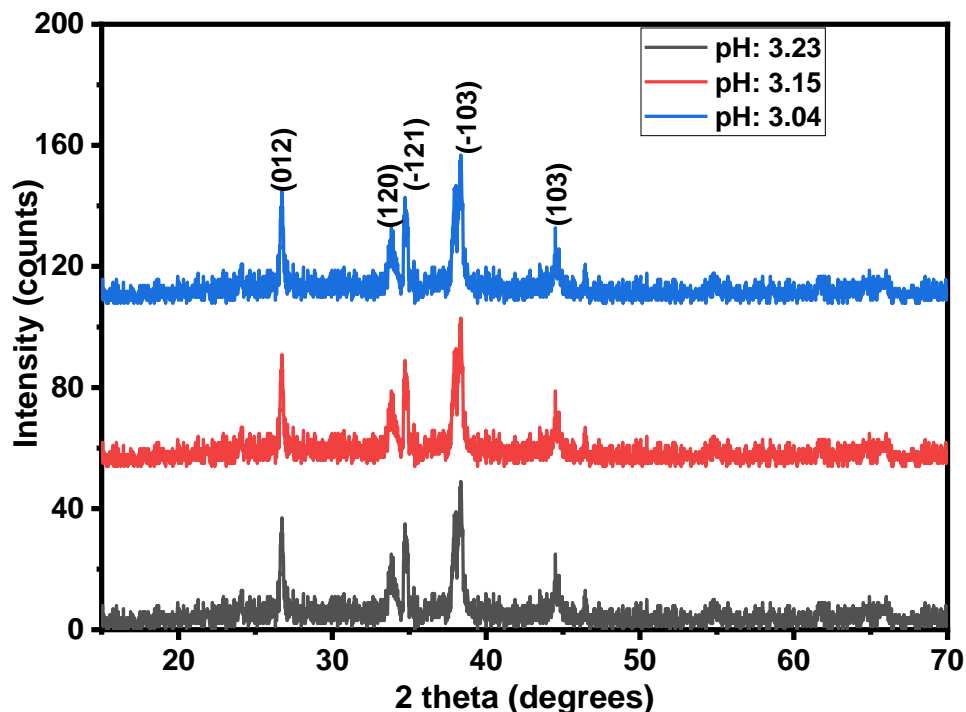


Figure4: Diffractogram of cerium doped Ag_2S deposited under different pH values

For the sample deposited at pH 3.23, the crystallite sizes range from 12.30 nm to 29.32 nm, with an average crystallite size of 20.39 nm. The micro-strain varies from 4.13×10^{-3} lines/nm² to 8.36×10^{-3} lines/nm² with an average strain of 6.46×10^{-3} . The dislocation density values range from 1.16×10^{-3} lines/nm² to 6.61×10^{-3} lines/nm², with an average strain of 3.40×10^{-3} lines/nm². These structural parameters suggest that deposition at this pH results in a mix of smaller and larger crystallites, influencing the overall crystal quality.

For the sample deposited at pH 3.15, the crystallite sizes range from 14.44 nm to 34.28 nm, with an average crystallite size of 22.96 nm. The micro-strain for this sample varies between 4.13×10^{-3} and 7.64×10^{-3} with an average micro-strain of 5.73×10^{-3} . The dislocation densities range from 0.85×10^{-3} lines/nm² to 4.80×10^{-3} lines/nm² with an average value of 2.59×10^{-3} lines/nm². Compared to the pH 3.23 sample, the pH 3.15 sample shows a slight increase in average crystallite size and a minor decrease in average dislocation density and strain, indicating an improvement in crystal quality with lower pH. The reduced micro-strain and dislocation density suggest a more relaxed crystal structure with fewer imperfections.

For the sample deposited at pH 3.04, the crystallite sizes range from 14.86 nm to 29.31 nm, with an average crystallite size of 23.29 nm. The micro-strain for this sample varies between 4.15×10^{-3} and 8.37×10^{-3} with an average micro-strain of 5.61×10^{-3} . The dislocation densities values range from 1.16×10^{-3} lines/nm² to $4. \times 10^{-3}$ lines/nm², with an average dislocation density of 2.34×10^{-3} lines/nm². The pH 3.04 deposition results in larger crystallite sizes and a moderate average dislocation density and strain among the three pH values, suggesting that the lowest pH tested leads to a good balance of structural properties. The slightly higher crystallite size and lower strain indicate improved crystal growth conditions at this pH. The obtained results in this study revealed good results which are comparable with results obtained by other researchers in literature. These results obtained suggest the possibility of using the material in optoelectronics devices like LEDs, solar cells, transducers, and photodetectors.

4.0. Conclusion

In this research, electro deposition of silver sulphide (Ag_2S) and cerium doped silver sulphide (Ce: Ag_2S) thin films for structural properties investigation has been carried out. Thin films of silver sulphide (Ag_2S) and cerium doped silver sulphide (Ce: Ag_2S) have been successfully deposited on conducting substrates (FTO) by electrodeposition method. Aqueous solutions of silver trioxonitrate (V), cerium tetraoxosulphate (VI) tetrahydrate, sodium thiosulphate, selenium (IV) oxide, tellurium (IV) oxide, were used as sources of silver, cerium, and sulphur.

Ethylene diamine tetra acetic acid (EDTA) and tetraoxosulphate (VI) acid were used as complexing agent and pH adjuster. Cerium ion was used as dopant introduced into silver sulphide. Three growth parameters such as dopant concentration (%), deposition time (duration) and pH of the electrolyte bath were optimized for the deposited thin films. Thin films obtained were characterized to determine their properties. The structural properties of the films obtained were studied using x-ray diffractometer. From the diffraction spectra obtained, 2 theta peaks, miller indices, d – spacing, crystallite sizes, dislocation densities and micro – strains of the deposited films were obtained. From the experimental investigation, increase in intensity of the diffraction spectra was observed as dopant concentration increased from 5% to 10%. The diffractogram exhibits distinct peaks corresponding to specific crystallographic planes, indicating changes in lattice parameters due to varying deposition times. The investigation also revealed that lowest pH tested leads to a good balance of structural properties. This study demonstrates that cerium doping enhances the structural properties of Ag₂S thin films by improving crystallinity, reducing lattice distortions, and promoting grain growth. Additionally, the research highlights the impact of deposition parameters (time, dopant concentration, and pH) on film quality, optimizing electrodeposition techniques for better material performance. Finally, the findings suggest that these doped thin films have promising applications in nanoelectronics, optoelectronics and next-generation energy technologies

5.0 Recommendation

Based on the experience gained and challenges encountered during the course of this work, the following are recommended for future research and government interventions.

- i. Use of other types of conducting substrate such as ITO, metal plates in electrodeposition of these films so as to determine the effect of the nature of the substrates on the properties of these films fabricated in this work. Also, use of non –conducting substrates should also be considered.
- ii. Exploring other properties of these films such as electrical, magnetic, supercapacitive, thermoelectric properties and electrochemical measurements to determine other possible area of applications like in, supercapacitor, thermoelectricity and electrodes for batteries.

Nomenclature

(Ce:Ag₂S) : cerium doped silver sulphide
Ce : Cerium

References

- Anbarasi, M., Nagarethinam, V. S., Baskaran, R., & Narasimman, V. 2016. Studies on the structural, morphological and optoelectrical properties of spray deposited CdS: Pb thin films. *Pacific Science Review A: Natural Science and Engineering*, 18(1), 72-77.
- N'guessan, A. I., Bouich, A., Soro, D., & Soucase, B. M. 2023. Growth of copper indium diselenide ternary thin films (CuInSe₂) for solar cells: Optimization of electrodeposition potential and pH parameters. *Heliyon*, 9(8).
- Hadri, A., Nassiri, C., Chafi, F. Z., Lohgmarti, M., & Mzerd, A. 2015. Effect of acetic acid adding on structural, optical and electrical properties of sprayed ZnO thin films. *Energy and Environment Focus*, 4(1), 12-17.
- Hwang, S. K., Yoon, J. H., & Kim, J. Y. (2024). Current status and future prospects of Kesterite Cu₂ZnSn (S, Se) 4 (CZTSSe) thin film solar cells prepared via electrochemical deposition. *ChemElectroChem*, 11(9), e202300729.
- Okoli, N. L., Ezenwaka, L. N., Okereke, N. A., Ezenwa, I. A., & Nwori, N. A. 2022. Investigation of Optical, Structural, Morphological and Electrical Properties of Electrodeposited Cobalt Doped Copper Selenide (Cu_{1-x}Co_xSe) Thin Films. *Trends in Sciences*, 19(16), 5686-5686.
- Mohapi, T. K. W., Yimamu, A. U., Tshabalala, K. G., & Motloug, S. J. 2023. Effect of deposition voltage on the properties of electrodeposited CdZrS thin films for solar cell application. *Physica B: Condensed Matter*, 671, 415405.
- Okorieimoh, C.C., Chime, U., Nkele, A. C., Nwanya, A. C., Madiba, I. G., Bashir, A. K. H., Botha, S., Asogwa, P. U., Maaza, M., and Ezema, F. I. 2019. Room-temperature synthesis and optical properties of nanostructured Ba-Doped ZnO thin films. *Superlattices and Microstructures*, 130, 321 – 331.
- Park, J., Seo, J., Lim, J. H., & Yoo, B. 2022. Synthesis of copper telluride thin films by electrodeposition and their electrical and thermoelectric properties. *Frontiers in Chemistry*, 10, 799305.
- Ravindranah, K., Prasad, K. D. V. and Rao, M. C. 2016. Spectroscopic and Luminescent Properties of Co²⁺ doped tin oxide thin film by Spray Pyrolysis. *Aims Material Science*, 3(3): 796 – 807.

- Read, D. T., & Dally, J. W. (1993). A new method for measuring the strength and ductility of thin films. *Journal of materials research*, 8(7), 1542-1549.
- Rodríguez-Rosales K., Marasamy L., Quiñones-Galván J., Santos-Cruz J., Mayén-Hernández S., Guillen-Cervantes A., Contreras- Puente G., 2020, de Moure-Flores F. One-step electrodeposition of CuAlGaSe₂ thin films using triethanolamine as a complexing agent, *Thin Solid Films*
- Ruiz-Gómez, S., Fernández-González, C., & Perez, L. 2022. Electrodeposition as a tool for nanostructuring magnetic materials. *Micromachines*, 13(8), 1223.
- Sawant, J. P., Bhujbal, P. K., Choure, N. B., Kale, R. B., & Pathan, H. M. 2022. Copper indium disulfide thin films: electrochemical deposition and properties. *ES Materials & Manufacturing*, 17(2), 14-22.
- Xue, J., Liu, J., Liu, Y., Li, H., Wang, Y., Sun, D., Wang, W., Huang, L. and Tang, J., 2019. Recent advances in synthetic methods and applications of Ag₂S-based heterostructure photocatalysts. *Journal of Materials Chemistry C*, 7(14), pp.3988-4003.
- Yadu G, K. K. Pathak, K. Deshmukh, and M. A. Pateria 2015 “Studies on optical and structural properties Of Ag₂S films prepared by chemical bath deposition method,” *International Journal of Multidisciplinary Research and Modern Education (IJMRME)*, vol.1, no. 1, pp. 296–301.
- Yimamu, A. U., Afrassa, M. A., Dejene, B. F., Echendu, O. K., Terblans, J. J., Swart, H. C., & Motloung, S. J. 2023. Electrodeposition of CdTe thin films using an acetate precursor for solar energy application: The effect of deposition voltage. *Materials Today Communications*, 35, 105673.
- Yu, Y., Gong, M., Dong, C., & Xu, X. 2023. Thin-film deposition techniques in surface and interface engineering of solid-state lithium batteries. *Next Nanotechnology*, 3, 100028.